# Nuclear Magnetic Resonance Solution Structure of PisI, a Group B Immunity Protein that Provides Protection Against the Type IIa Bacteriocin Piscicolin 126, PisA[†,‡]

Leah A. Martin-Visscher,[§] Tara Sprules,[||] Lucas J. Gursky,[§] and John C. Vederas*[,§]

*Department of Chemistry, University of Alberta, Edmonton, Alberta, Canada T6G 2G2, and Quebec/Eastern Canada High Field NMR Facility, McGill University, Montreal, Quebec, Canada H3A 2A7*

*Received March 7, 2008; Revised Manuscript Received April 6, 2008*

ABSTRACT: Lactic acid bacteria produce and secrete bacteriocins. These bacteriocins are potent antimicrobial peptides that are active against other closely related bacteria. As a means of self-protection, producer organisms also express immunity proteins. Immunity proteins are generally located on the same genetic locus and are cotranscribed with the bacteriocin. Although some cross immunity between bacteriocins has been observed, immunity proteins are typically highly specific. Immunity proteins for the type IIa bacteriocins range from 81 to 115 amino acids in length and display substantial variation in their sequences. Nonetheless, such immunity proteins have been classified into three groupings (groups A, B, and C) according to sequence homology. The structures of a group C (ImB2) and two group A (EntA-im and PedB) immunity proteins have previously been reported. We herein report the nuclear magnetic resonance solution structure of the remaining class of the type IIa immunity proteins. PisI, a 98-amino acid protein, is a group B immunity protein conferring immunity against piscicolin 126 (PisA). Like ImB2, EntA-im, and PedB, PisI folds into a globular protein in aqueous solution and contains an antiparallel four-helix bundle. Compared to ImB2 and EntA-im, PisI has a substantially longer and more flexbile N-terminus, but a shorter C-terminus. No direct interaction between the bacteriocin and immunity protein is observed by NMR in either aqueous or membrane mimicking environments. This further suggests that the mechanism that mediates immunity is not due to a direct bacteriocin−immunity protein interaction but rather is receptor-mediated. It has now been confirmed that the four-helix bundle is indeed a structural motif among the type IIa immunity proteins.

Bacteriocins are ribosomally synthesized antimicrobial peptides. Lactic acid bacteria (LAB)[1] produce a variety of bacteriocins that are active against closely related species, including food-borne pathogens such a *Listeria monocytogenes*. In general, these bacteriocins exhibit no toxicity to human or eukaryotic cells. As such, there is extensive research into the potential of these bacteriocins for use in food preservation and as human therapeutics (*1–4*). The type IIa, or pediocin-like, bacteriocins make up an important class of antimicrobial peptides produced by LAB. The first type IIa bacteriocin to be purified and fully characterized was leucocin A (*5*). To date, more then 30 type IIa bacteriocins have been identified (*2*). These heat stable peptides are small (37−48 residues), cationic, and highly antilisterial. There is a high degree of sequence homology in the N-terminal domain of these peptides, characterized by the consensus sequence YGNGVXC and a conserved disulfide bridge (*2, 3, 6, 7*). The three-dimensional solution structures of four type IIa bacteriocins (leuA, CbnB2, curvacin A, and two sakacin P variants) have been reported (*8–11*). These structures reveal that in membrane mimicking environments, the cationic N-terminus assumes a $\beta$-sheet structure, whereas the hydrophobic and/or amphiphilic C-terminal end of the peptide is α-helical. The far C-terminus folds back over the helix with a hairpin loop. The two domains of the bacteriocin are connected by a hinge region, which allows them to move relative to each other (*2, 4, 8, 10, 11*). Subsequent modeling studies of a variety of other type IIa bacteriocins have confirmed this structural pattern among the type IIa bacteriocins (*12, 13*). Studies involving mutations to this class of bacteriocins, as well as hybrid bacteriocins, have shown

[†] These studies were supported by the Natural Sciences and Engineering Research Council of Canada (NSERC), the Alberta Heritage Foundation for Medical Research (AHFMR), and the Advanced Food and Materials Network (AFMNet).

[‡] Atomic coordinates for PisI have been deposited in the Protein Data Bank as entry 2K19. Chemical shifts have been deposited in the BioMagResBank as entry 15673.

* To whom correspondence should be addressed. Telephone: (780) 492-5475. Fax: (780) 492-2134. E-mail: john.vederas@ualberta.ca.

[§] University of Alberta.

[||] McGill University.

[1] Abbreviations: LAB, lactic acid bacteria; PisI, piscicolin 126 immunity protein; PisA, bacteriocin piscicolin 126; ImB2, carnobacteriocin B2 immunity protein; EntA-im, enterocin A immunity protein; PedB, pediocin PP-1 immunity protein; man-PTS and $EII_t^{man}$, mannose phosphotransferase system; OD, optical density; MBP, maltose binding protein; EDTA, ethylenediaminetetraacetic acid; $NaN_3$, sodium azide; DTT, dithiothreitol; AEBSF, 4-(2-aminoethyl)benzenesulfonyl fluoride; MALDI-TOF, matrix-assisted laser desorption ionization time-of-flight; HSQC, heteronuclear single-quantum coherence; NOE, nuclear Overhauser effect; rmsd, root-mean-square deviation; TFE, trifluoroethanol; CD, circular dichroism.

10.1021/bi8004076 CCC: $40.75 
Published on Web 05/24/2008

that the antimicrobial specificity is governed by the C-terminal domain of the bacteriocin (*13–18*).

Bacteriocins are generally are co-expressed with their cognate immunity proteins (*19, 20*). Although some cross immunity has been observed (*19, 21*), immunity proteins are highly specific, ensuring that the producer organism is protected from its own bacteriocin (*2–4, 19*). While there is high degree of sequence homology between the type IIa bacteriocins, the same is not true for their immunity proteins. The type IIa immunity proteins range in size from 81 to 115 amino acids, and the level of sequence homology varies from 5 to 85% (*19*). As with the bacteriocins, studies on hybrids of the type IIa immunity proteins suggest that the C-terminal domain of the protein confers immunity and is involved in specific recognition with its cognate bacteriocin (*12, 18*). The mechanism of immunity is not fully understood. It has been shown that the activity of the type IIa bacteriocins is receptor-mediated (*22*), and it is believed that this receptor is part of the mannose phosphotransferase system ($EII_t^{man}$) (*23–27*). It has therefore been hypothesized that immunity proteins also interact with this system, either by preventing the bacteriocin from binding to it, by blocking pore formation, or perhaps by directly interacting with the bacteriocin (*19, 24, 28, 29*).

The type IIa immunity proteins have been classified into three groups, according to sequence homology (*19*) (Figure 1). To date, structures from two of these classes have been reported. In 2004, we published the NMR solution structure of ImB2, a group C immunity protein. Our work revealed that under aqueous conditions this protein assumes a well-defined structure with an antiparallel four-helix bundle. The helices are nearly parallel with each other, resulting in tight packing and the formation of a hydrophobic core in the center of the protein. A large, flexible loop connects α3 and α4. The C-terminus contains a fifth helix and an extended strand, which runs perpendicular to α3 and α4 (*30*). Subsequently, the structures of two group A immunity proteins (EntA-im and PedB) were reported (*31, 32*). Like ImB2, these proteins contain an antiparallel four-helix bundle. However, in EntA-im and PedB, the loop between α3 and α4 is more clearly defined. Residues from this loop are incorporated into the hydrophobic core, and α3 and α4 acquire a triangular relationship relative to each other. In the absence of a fifth helix and extended C-terminus, the third helices of EntA-im and PedB are straight, rather than kinked (as observed for α3 in ImB2) (*32*).

In this study, we report the three-dimensional structure of PisI, a group B type IIa immunity protein that confers immunity to piscicolin 126 (*33, 34*). The NMR solution structure of this 98-amino acid protein reveals that is it comprised of a four-helix bundle, similar to the reported structures of ImB2, EntA-im, and PedB. The structure of this group B immunity protein now confirms that the four-helix bundle is a common structural motif for the type IIa immunity proteins.

## MATERIALS AND METHODS

*Bacterial Strains and Culture Conditions.* Bacterial strains and plasmids used in this study are described in Table SI of the Supporting Information. *Carnobacterium maltaromaticum* UAL26 and *Carnobacterium divergens* LV13 were grown in APT broth as previously described (*33*). For cloning experiments and overexpression in unlabeled media, *Escherichia coli* K12 TB1 and BL21(DE3) cultures were grown in Luria-Bertani (LB) broth at 37 °C and 200 rpm or on LB agar at 37 °C. For overexpression experiments involving labeled media, *E. coli* K12 TB1 cultures were grown in Celtone-CN rich medium (Spectra Stable Isotopes) and *E. coli* BL21(DE3) cultures were grown in isotopically enriched M9 minimal medium (see the Supporting Information for the recipe) at 37 °C and 200 rpm. Medium containing ampicillin (100 μg/mL) was used for selection of transformants. Stock cultures of *C. maltaromaticum* UAL26, *C. divergens* LV13, and *E. coli* were maintained at −78 °C in APT broth and LB broth with 20% glycerol.

*Construction of malE−pisI and malE−pisA Fusions.* Genomic template DNA was prepared from *C. maltaromaticum* UAL26 using the DNeasy tissue isolation kit (Qiagen). Both PisA and PisI genes were amplified with PCR, using the appropriate primers (Table SII of the Supporting Information) following standard protocol. Only the DNA encoding the mature part of piscicolin 126 was amplified. The resulting PCR products were purified with the QiaQuick PCR purification kit (Qiagen) and subjected to agarose gel electrophoresis to confirm the correct size. pMAL-PisA and pMAL-PisI were constructed by cloning the PCR products containing *pisA* and *pisI* into pMAL-c2x (New England Biolabs) as follows. The PCR products were first trimmed with T4 polymerase (Invitrogen) and dNTPs (Invitrogen) to remove 3′ overhangs and then digested with HindIII. pMAL-c2x was simultaneously digested with XmnI and HindIII. DNA manipulation and transformation of the resulting plasmids into *E. coli* K12 TB1 were carried out according to the manufacturer's protocol (New England Biolabs). The DNA inserts were sequenced using the primers LGMALE and LGM13PUC (Table SII of the Supporting Information) and fluorescent dideoxy-chain terminators (Amersham DYEnamic ET kit) and analyzed on a 3730 DNA analyzer (Applied Biosystems). The recombinant plasmids were isolated and transformed into *E. coli* BL21(DE3) competent cells (Stratagene) according to the manufacturer's protocol.

*Purification of [$^{13}$C,$^{15}$N]PisI and [$^{15}$N]PisI.* Initial production of the $^{13}$C- and $^{15}$N-labeled fusion protein was achieved by growing *E. coli* K12 TB1, transformed with the pMAL-PisI plasmid, in [$^{13}$C,$^{15}$N]Celtone-CN rich medium. However, this host strain was not amenable to growth in minimal medium. Therefore, *E. coli* BL21(DE3) cells were transformed with the same plasmid, producing a clone capable of growth in M9 minimal medium, utilizing $(^{15}NH_4)_2SO_4$ and [U-$^{13}$C]-D-glucose (99% isotopic purity, Cambridge Isotope Laboratories) as the sole nitrogen and carbon sources, respectively. In either case, the cells were grown at 37 °C and 200 rpm, in the appropriate medium, containing 100 μg/mL ampicillin. When the $OD_{600}$ of the cell culture reached 0.5, overexpression of the recombinant protein was induced by the addition of isopropyl β-D-thiogalactopyranoside to a final concentration 0.3 mM. The culture was incubated for an additional 3 h. The cells were then harvested by centrifugation, resuspended in amylose column buffer [20 mM Tris-HCl (pH 7.4), 200 mM NaCl, 1 mM EDTA, 1 mM $NaN_3$, and 1 mM DTT] and subsequently stored at −78 °C. Cell lysis was achieved by the addition of lysozyme (0.1 mg/mL) and three consecutive freeze−thaw cycles, followed

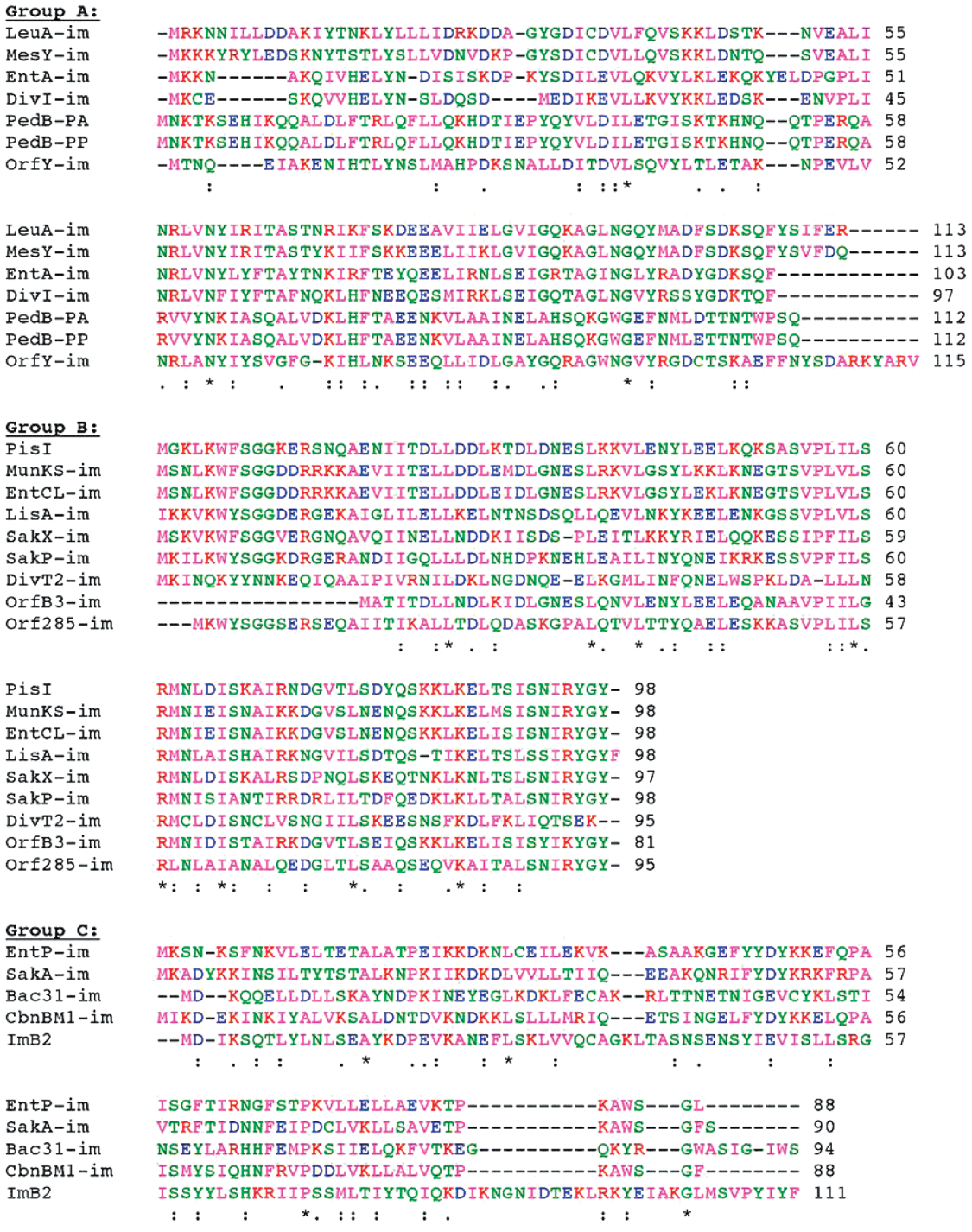


FIGURE 1: Sequence alignment of (putative) immunity proteins for various type IIa bacteriocins. Sequences were aligned using ClustalW (*46*) and arranged into groups according to the work of Fimland et al. (*19*). Group A: immunity proteins for leucocin A (*5*), mesentericin Y105 (*47*), enterocin A (*48*), divercin V41 (*49*), pediocin PA-1 (*49*), pediocin PP-1 (*32*), and an orphan immunity protein with no corresponding bacteriocin, OrfY-im (*50*). Group B: immunity proteins for piscicolin 126 (*33*), muntdicin KS (*51*), enterocin CRL35 (*52*), listeriocin 743A (*53*), sakacin 5X (*54*), sakacin P (*55*), an orphan immunity protein with no corresponding bacteriocin (DivT2-im) (*49*), an orphan immunity protein with no corresponding bacteriocin (OrfB3-im) (*56*), and an orphan immunity protein with no corresponding bacteriocin (Orf285-im) (*57*). Group C: immunity proteins for enterocin P (*58*), sakacin A (*59*), bacteriocin 31 (*60*), carnobacteriocin BM1, and carnobacteriocin B2 (*56*). Amino acids are colored according to physicochemical characteristics as follows: blue for acidic, red for basic, magenta for hydrophobic, and green for polar (and glycine). Conserved residues are denoted with an asterisk, conservative substitutions with a colon, and semiconservative substitutions with a period.

by sonication. The resulting solution was centrifuged, and the lysate was applied to a column of amylose resin (New England Biolabs). The column was washed with amylose column buffer, and the fusion protein was eluted with column buffer containing 10 mM maltose, according to the manufacturer's protocol. The resulting protein solution was dialyzed against water, lyophilized, and stored at −78 °C until further use. PisI was cleaved from MalE using Factor Xa. Factor Xa (0.5%, w/w) was added to a 1 mg/mL solution of the fusion protein in column buffer [20 mM Tris-HCl (pH 8.0), 100 mM NaCl, and 2 mM $CaCl_2$]. The mixture was allowed to digest at room temperature for 18 h. AEBSF was

then added to the solution (final concentration of 0.1 mM) to irreversibly inhibit the enzyme and prevent secondary cleavage. PisI was purified with cation-exchange chromatography using SP Sepharose (Pharmacia), followed by RP-HPLC, using a C18 column. See the Supporting Information for cation-exchange and HPLC methods. The purity of the peptide was assessed by MALDI-TOF spectrometry. The purified peptide was lyophilized and stored at −78 °C.

*Purification of [$^{15}$N]PisA.* *E. coli* BL21(DE3) cells harboring the pMAL-PisA plasmid were grown at 37 °C and 200 rpm in M9 minimal medium containing 100 $\mu$g/mL ampicillin and $(^{15}NH_4)_2SO_4$ as the sole nitrogen source. Overexpression and purification of the MalE−PisA fusion protein were carried out in the same manner as previously described for the MalE−PisI fusion protein. During the cleavage of PisA from MalE with Factor Xa, it was discovered that PisA precipitated out of solution. Thus, the salt concentration of the Factor Xa buffer solution was increased to 150 mM NaCl. The fusion protein was dissolved (1 mg/mL) in buffer, and 0.5% (w/w) Factor Xa was added. Digestion was complete after 8 h at room temperature, with gentle stirring. AEBSF was then added to inhibit the enzyme and prevent secondary cleavage. The peptide was purified by RP-HPLC, using a C18 column (see the Supporting Information). The purity of the peptide was assessed by MALDI-TOF spectrometry. The purified peptide was lyophilized and stored at −78 °C.

*NMR Spectroscopy of [$^{15}$N]PisI and [$^{13}$C,$^{15}$N]PisI.* NMR samples contained ~0.5 mM protein in a 90% $H_2O$/10% $D_2O$ mixture or 100% $D_2O$, 20 mM sodium phosphate (pH 5.9), 1 mM EDTA, 1 mM $NaN_3$, and 50 $\mu$M 2,2-dimethyl-2-silapentane-5-sulfonate sodium salt (DSS). NMR spectra were recorded at 25 °C on Varian Inova 500 and 800 MHz spectrometers equipped with triple-resonance HCN cold probes and $z$-axis pulsed-field gradients (PFGs). The following experiments were used for backbone and side chain $^1$H, $^{13}$C, and $^{15}$N resonance assignments: $^{15}$N HSQC, $^{15}$N HSQC-TOCSY, $^{15}$N HSQC-NOESY, HNHA, HNCACB, CBCA(CO)NH, C(CO)NH, $^{13}$C HSQC, $^{13}$C HCCH-TOCSY, $^{13}$C HCCH-COSY, and $^{13}$C HSQC-NOESY. NMR spectra were processed using NMRPIPE and analyzed with NMRView (*35, 36*). Data were multiplied by a 90°-shifted sine-bell squared function in all dimensions. Indirect dimensions were doubled by linear prediction and zero-filled to the nearest power of two prior to Fourier transformation. Additional details are provided in the Supporting Information.

*Structure Calculations.* NOE restraints were obtained from the $^{15}$N- and $^{13}$C-edited HSQC-NOESY experiments, and $\phi$ angle restraints were derived from analysis of the diagonal peak to cross-peak intensity ratio in the HNHA experiment. The structure of PisI was calculated by using the CANDID module in CYANA 2.1 (*37*), using a combination of manually and automatically assigned NOEs (manual inspection of the peaks was necessary due to the presence of degraded material). Peaks were calibrated according to their intensities. A family of 100 random structures was generated and subjected to simulated annealing, with 10000 torsion angle dynamic steps. After seven rounds of calculation, 2627 of the initial 2915 peaks were assigned. After accounting for symmetric peaks, a total of 1725 upper distance restraints and 76 $\phi$ dihedral angles were used in the final round of calculations. The 20 lowest-energy conformations (no NOE violations of >0.3 Å with no residues in the disallowed region of the Ramachandran plot) were chosen as being representative of the solution structure of PisI. The backbone rmsd for residues 13−92 was 0.56 Å. Structural statistics were calculated with CYANA and MOLMOL (*38*). Figures were generated with PyMOL (http://www.pymol.org), PDB2PQR (*39*), APBS (*40*), and MOLMOL. Coordinates have been deposited in the Protein Data Bank (http://www.rcsb.org/pdb), as entry 2K19. Chemical shift assignments have been deposited in BMRB as entry 15763 (http://www.bmrb.wisc.edu/). Additional details are provided in the Supporting Information.

*Titration of [$^{15}$N]PisA with PisI.* [$^{15}$N]PisA was dissolved in the same buffer used for the NMR studies of PisI (described above). The $^{15}$N HSQC spectrum of [$^{15}$N]PisA was recorded in the presence of 0, 0.5, 1.0, and 2.0 molar equiv of unlabeled PisI. Spectra were acquired at 25 °C on a Varian Inova 600 MHz spectrometer. To induce helicity in the C-terminal region of the bacteriocin, PisA was dissolved in a 1:1 mixture of trifluoroethanol and aqueous buffer as follows. [$^{15}$N]PisA was initially dissolved in aqueous buffer [40 mM sodium phosphate (pH 6.0), 2 mM EDTA, 2 mM $NaN_3$, and 100 $\mu$M DSS]. An equivalent volume of $d_3$-TFE was then added. The concentration of [$^{15}$N]PisA was estimated to be 0.6 mM by UV absorbance at 280 nm. The $^{15}$N HSQC spectrum of [$^{15}$N]PisA was recorded in the presence of 0 and 1.1 molar equiv of unlabeled PisI (also prepared in a 1:1 TFE/aqueous buffer mixture).

*Protein Concentration.* Protein concentrations were determined by measuring the UV absorption at 280 nm. The molar extinction coefficients for the proteins were calculated using ProtParam (*41*) available on the ExPASY database (http://expasy.org).

## RESULTS

*Chemical Shift Assignment of PisI.* PisI is a 98-amino acid protein, with 15 leucines, 7 isoleucines, 12 lysines, and 11 serines (comprising 46% of the protein). To facilitate NMR studies, this protein was overexpressed as a maltose-binding fusion protein and grown in either $^{13}$C- and $^{15}$N-enriched medium or $^{15}$N-enriched medium. The fusion protein was purified over an amylose column and subsequently cleaved with Factor Xa. PisI was purified by cation-exchange chromatography, followed by RP-HPLC. The amide cross-peaks in the $^{15}$N HSQC spectrum of PisI are relatively well dispersed, despite the high degree of multiplicity (Figure 2). Although there is some overlap, all of the expected amide protons could be assigned, except for the first two residues, which could not be observed due to rapid exchange with solvent. Sequential backbone and C$\alpha$ and C$\beta$ chemical shift assignments for PisI were obtained by analysis of HNCACB and CBCA(CO)NH spectra. Further side chain assignments were made by analysis of CCONH, $^{15}$N HSQC-TOCSY, $^{13}$C HCCH-TOCSY, and $^{13}$C HSQC experiments. Almost complete backbone and side chain $^1$H, $^{15}$N, and $^{13}$C assignments were obtained (~99%, with 96 of 98 residues fully assigned). Secondary chemical shift analysis of the assigned $\alpha$- and $\beta$-carbons indicated that PisI was highly structured and likely contained four distinct helices (data not shown) (*42*).

*Structure of PisI.* A family of 20 structures, representative of the solution structure of PisI, was obtained using CYANA

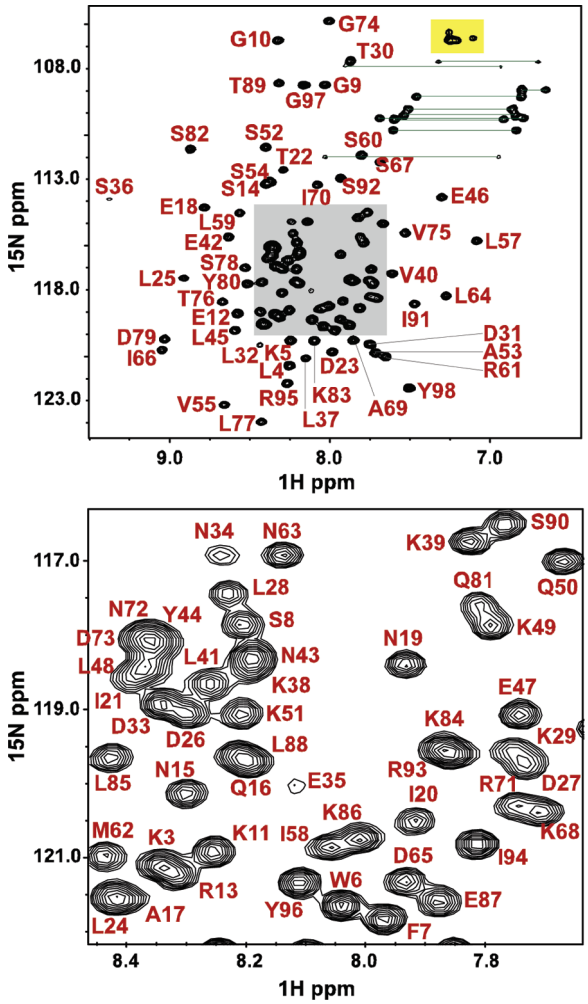


FIGURE 2: $^{15}$N HSQC spectrum (800 MHz) of PisI in 20 mM sodium phosphate (pH 5.9) at 25 °C. Cross-peaks from Asn and Gln side chains are indicated with horizontal lines; those from Arg are highlighted in yellow, and the Trp side chain is not shown. All other cross-peaks are labeled by residue number. The top panel shows the full spectrum. The gray box is enlarged in the bottom panel for clarity.

Table 1: Structural Statistics for PisI

| | |
|---|---|
| distance restraints | |
| total no. of NOE restraints | 1725 |
| intraresidual ($i - j = 1$) | 553 |
| short ($i - j \leq 1$) | 442 |
| medium ($1 < i - j < 5$) | 444 |
| long ($i - j \geq 5$) | 286 |
| no. of $\phi$ angles | 76 |
| average target function value | 1.83 ± 0.14 |
| rmsd (Å) for residues 13−92 | |
| backbone | 0.56 ± 0.10 |
| heavy atoms | 1.03 ± 0.12 |
| Ramachandran plot | |
| most favored (%) | 83.9 |
| allowed (%) | 16.1 |
| additionally allowed (%) | 0 |
| disallowed (%) | 0 |

2.1. The structural statistics characterizing these structures are summarized in Table 1. As shown in Figure 3, the final ensemble of 20 structures is well-defined between residues R13 and N92. PisI consists of a four-helix bundle, flanked by a flexible N-terminus and slightly more rigid C-terminus. Heteronuclear NOE data show an average NOE of 0.75 from residues S14−S91, which would be expected for a structured,

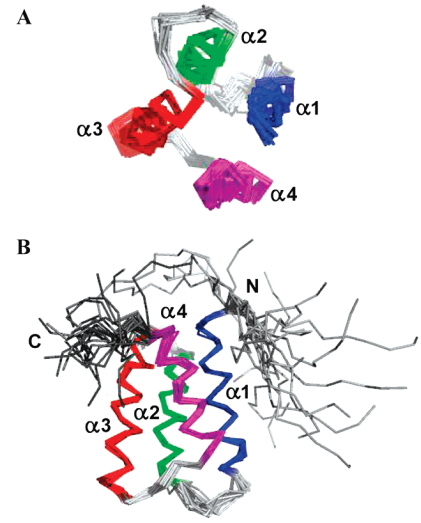


FIGURE 3: Superposition of the 20 lowest-energy structures on the backbone of the α-helices. Helices 1−4 are labeled and colored blue, green, red, and magenta, respectively. (A) Looking down the axis of the helix. The N- and C-termini have been omitted for clarity. (B) A 90° rotation into the plane of the paper shows the side view of the structure. The N- and C-termini are labeled and colored gray.

globular protein (data not shown). This value is slightly smaller for certain residues in the loops connecting the helices, but overall, the loops are also relatively rigid. The N-terminus of the protein is quite mobile, as evidenced by negative NOE values for residues K3−K5, and values of <0.5 for residues W6−K13. The helices of PisI are relatively straight and range in length from 12 to 19 amino acids. α1 is formed by residues R13−K29, α2 by residues K38−K49, α3 by residues V55−D73, and α4 by residues D79−I92. Angles of 28°, 7°, 32°, and 15° are found between the pairs formed by α1 and α2, α2 and α3, α3 and α4, and α4 and α1, respectively. The hydrophobic side chains of the helices pack tightly and form the interior of the four-helix bundle, as evidenced by numerous interhelical NOEs. Most polar and hydrophilic residues face the aqueous exterior (Figure 4A).

*Titration of [$^{15}$N]PisA with PisI.* NMR was used to monitor the interaction between the bacteriocin PisA and its immunity protein, PisI. Under aqueous conditions, PisA is unstructured, as evidenced by CD spectroscopy (see Figure S1 and Table S1 of the Supporting Information). The titration of PisI with [$^{15}$N]PisA did not cause significant changes in the $^{15}$N HSQC spectrum. We repeated the experiments under membrane mimicking conditions. The addition of 50% TFE induces helicity in PisA, as evidenced by the CD data (see Figure S1 and Table S1 of the Supporting Information) and by the change in spectral dispersion of the amide cross-peaks in the $^{15}$N HSQC spectrum of PisA, compared to aqueous conditions. However, addition of immunity protein did not result in any further change in the spectrum of PisA.

## DISCUSSION

*Structure of PisI.* To confirm that PisI is the cognate immunity protein for piscicolin 126 (PisA), we have heterologously expressed PisI in PisA-sensitive host, such as *C. maltoaromaticum* LV17C and *C. divergens* LV13. The transformed strains show complete loss of sensitivity to PisA

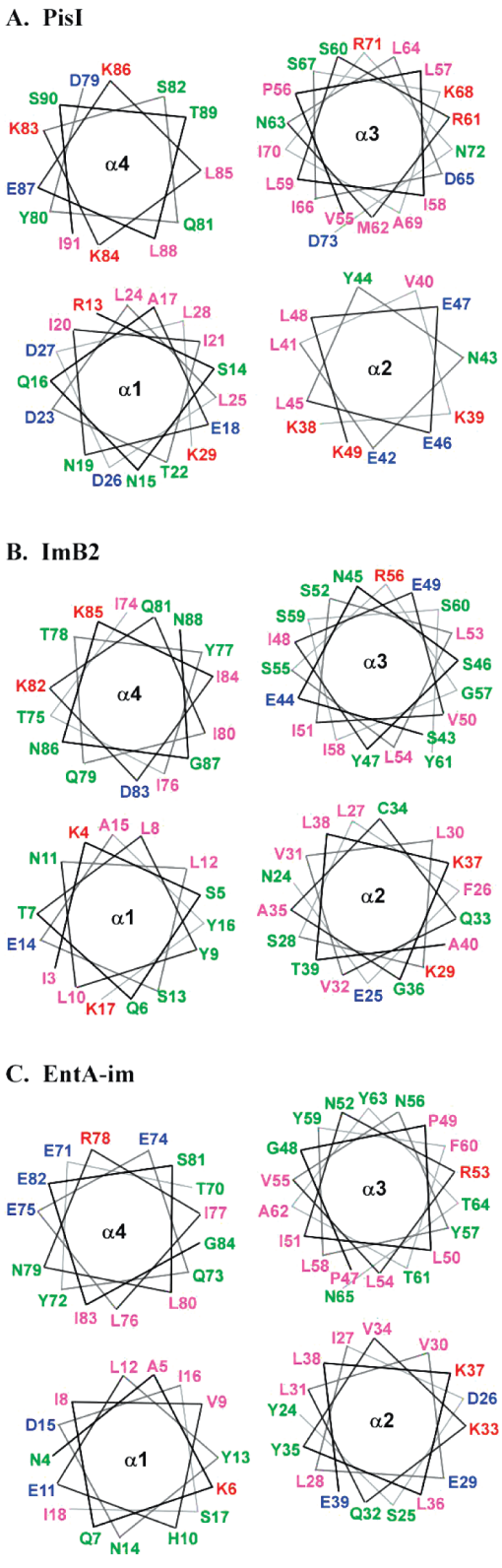


FIGURE 4: Helical wheel diagrams of (A) PisI, (B) ImB2, and (C) EntA-im. The helices are labeled and arranged in approximately the same orientation as seen when looking down the axis of the four-helix bundle. Helix 5 of ImB2 has been omitted. Residues are labeled and colored as follows: blue for acidic, red for basic, magenta for hydrophobic, and green for polar (and glycine).

compared to the control, verifying that PisI imparts immunity to PisA (data not shown). The NMR solution structure of PisI reveals that it folds into an antiparallel four-helix bundle, with a long, flexible N-terminus and a shorter, more rigid

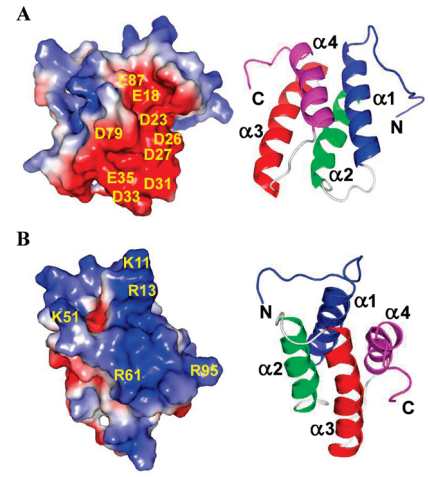


FIGURE 5: Electrostatic surface potential of PisI. A ribbon diagram is shown for reference, and the termini and helices are colored and labeled: (A) viewing the negatively charged region and (B) viewing the positively charged region. Blue indicates positive charge and red negative charge. Key residues are identified.

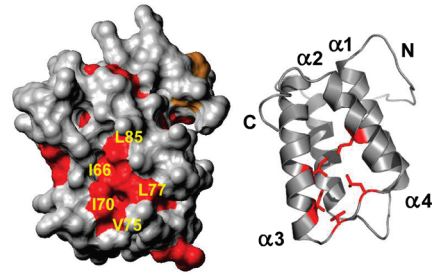


FIGURE 6: Hydrophobic surface of PisI. A ribbon diagram is shown for reference, and the termini and helices are labeled. In the surface plot, red indicates hydrophobicity from Ile, Leu, and Val. Key residues are labeled on the surface plot and colored red in the ribbon diagram.

C-terminus. There are also some unique surface features that can be identified. PisI has both negatively and positively charged regions. The large, negatively charged groove is formed by residues in α1 (E18, D23, D26, and D27) and α4 (D79 and E87) and extends down to the loop between α1 and α2 (D31, D33, and E35) (Figure 5A). Many of these residues are conserved among the group B immunity proteins (Figure 1). The positively charged patch is located at the junction of the N-terminus of α1 (K11 and R13), the loop connecting α2 and α3 (K51), R61 of α3, and the C-terminus of α4 (R95) (Figure 5B). Like the negatively charged region, several of these residues are also conserved within the group B immunity proteins, particulary R13, R61, and R95 (Figure 1). PisI also has a small, hydrophobic pocket, located near the connecting loop of α3 and α4 (Figure 6). This pocket is comprised of I66, I70, V75, L77, and L85. All of these residues are very highly conserved in the group B immunity proteins (Figure 1). Since protein−protein interactions generally involve hydrophobic interactions, this region may be involved in the interaction between the immunity protein and its receptor. Sequence alignment shows that of the three groups of immunity proteins, the group B proteins are most similar in sequence (Figure 1). It is therefore likely that the structure of PisI is representative of the other group B immunity proteins.

*Comparison of Group B Immunity Proteins to Group A and C Immunity Proteins.* The structures of three type IIa

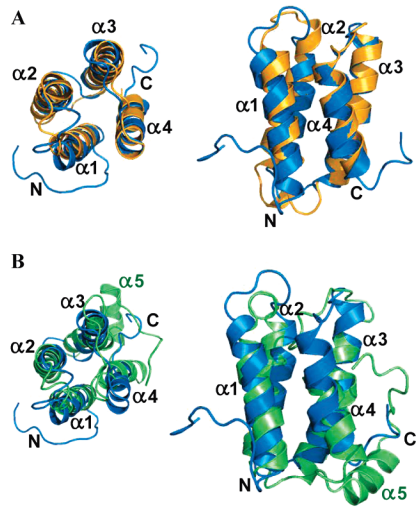


FIGURE 7: Superposition of PisI (blue) with EntA-im (orange) and ImB2 (green). The diagram on the left shows the view down the axis of the bundle and the diagram on the right illustrates the helical overlap of the proteins. The N- and C-termini and helices are labeled. (A) PisI and EntA-im. (B) PisI and ImB2.

immunity proteins have previously been reported. ImB2 belongs to subgroup C, whereas EntA-im and PedB both belong to subgroup A. By comparing the structure of PisI to ImB2 and EntA-im, it is apparent that there are both similarities and differences among these three subgroups.

The four-helix bundle is a conserved motif among the type IIa immunity proteins. PisI, along with the group A and C immunity proteins, consists of a four-helix bundle which folds around a hydrophobic core. Despite the low degree of sequence homology between PisI and ImB2 (13%) and EntA-im (17%), the four-helix bundle of PisI overlaps very well with these proteins (Figure 7). The backbone rmsd value for the alignment of PisI to ImB2 and PisI to EntA-im is 1.9 and 1.5 Å, respectively. Inspection of the helical wheel diagrams of PisI, ImB2, and EntA-im shows that for each protein, the core of the four-helix bundle is comprised of hydrophobic side chains, whereas hydrophilic and polar side chains reside on the exterior surface of the protein. There are slight variations in the position of charged and exposed hydrophobic residues between the three subgroups (Figure 4), but overall, the architecture of the four-helix bundle is very similar.

Recently, it has been proposed that the group A and C immunity proteins can be distinguished on the basis of differences in their three-dimensional structures. It was suggested that the absence of a fifth helix, as well as the straightened loop connecting α3 and α4, in the group A immunity proteins was a feature unique to this subclass (*32*). However, the structure of PisI (group B) contradicts this claim. Like EntA-im and PedB (both group A), PisI lacks a fifth helix. The connecting loops between the helices in PisI are all well-defined. In fact, PisI overlays just as well with both EntA-im (1.5 Å) and PedB (1.4 Å) as EntA-im and PedB overlay with each other (1.3 Å). Furthermore, the interhelical angle between α3 and α4 of PisI is ~32°, which is almost identical to the angle of 30° reported for the same helical pair in PedB. Like PedB, PisI also has two hydrophobic residues (V75 and L77) in the connecting loop between α3 and α4 that are aligned in the interhelical space and participate in formation of the hydrophobic core. These findings suggest that the four-helix bundle is highly conserved between the group A and B immunity proteins, and these subclasses cannot be distinguished on a structural basis. The observed differences between ImB2 and the group A and B immunity proteins are most likely a result of ImB2 being atypical. ImB2 is significantly longer than any other group C immunity protein. As such, it is unlikely that the other group C immunity proteins would contain a fifth helix. Although some group A immunity proteins are similar in length to ImB2 (such as LeuA-im, MesY-im, and PedB), the structures of EntA-im and PedB show no electron density in the C-terminal region of the protein, indicating that this region is unstructured. Thus, the presence of a fifth helix appears to be unique to ImB2. It is interesting to note that the cognate bacteriocin, carnobacteriocin B2, is the longest (48 amino acids) of the type IIa peptides.

There are many similarities in the surface features of the group A, B, and C immunity proteins. Like PisI, the structure of EntA-im is reported to have a negatively charged patch (*31*). Although the participating residues are slightly different, the relative location of this patch is very similar to that of PisI. Structural models for several other group A immunity proteins, including two hybrid proteins, are also predicted to display this negative region (*31*). The positively charged region is also common to all three subgroups. For the group A immunity proteins (EntA-im and PedB), this region is formed by residues in α2 and α3 and the connecting loop between these helices (*31, 32*). For the group C immunity protein ImB2, this region is located in the flexible loop connecting α3 and α4 (*30*). Although the position of this patch varies among the three subclasses, the presence of such a region is conserved and in all cases is located in the C-terminal half of the protein. It has been suggested that this region may be involved in attracting the immunity protein to the surface of the cell membrane (*30*).

As previously discussed, PisI has a small hydrophobic pocket. The group C immunity protein, ImB2, also displays such a patch, albeit in a different location. In ImB2, this pocket is formed by hydrophobic residues in α2 and α3. Sequence alignment shows that the group A immunity proteins have hydrophobic residues corresponding to the same location in ImB2 and, therefore, likely display a hydrophobic pocket in this region. It has been suggested that this hydrophobic patch may mediate protein−protein interaction between the immunity protein and its putative receptor (*30*). Since all three subclasses exhibit this hydrophobic patch, this region may be critical for imparting immunity.

The most prominent difference between PisI and the other type IIa immunity proteins is the length and flexibility of both the N- and C-termini. PisI has a longer, more flexible N-terminus compared to the group A and C immunity proteins. On the other hand, the C-terminus of PisI is significantly shorter. Both the N- and C-termini of PisI contain several polar or charged residues that are well-conserved within the group B immunity proteins. Studies involving hybrid immunity proteins (*18, 19*), as well as shortened variants of PedB (*32*), suggest that the C-terminal portion (extreme C-terminus in the case of PedB) of the protein is involved in specific recognition. However, this work has only used immunity protein and hybrids derived from subgroup A. Since PisI shows such a marked difference in its N-terminus, this region may also be involved in

recognition. In fact, two residues in the N-terminus (K11 and R13) contribute to the positively charged patch of the protein. If this patch helps attract the protein to the cell membrane, then the N-terminus of the protein may also be crucial for recognition. Sequence alignment of the group B immunity proteins shows that this region is highly conserved. To investigate the importance of the N-terminus, the effect of mutations to the N- and C-termini of the group B immunity proteins will need to be studied. Alternatively, hybrid proteins involving the group B immunity proteins may shed light on the role of the N-terminus.

*Lack of Direct Interaction between PisA and PisI.* The mechanism of action between the type IIa immunity proteins and their bacteriocins is not well understood. Various experimental approaches have been used to probe this interaction. Quadri et al. detected no binding between ImB2 and microtiter plates coated with CbnB2 (*43*). Several groups have observed that the extracellular addition of immunity protein in the presence of bacteriocin did not confer protection to sensitive strains, whereas heterologous expression of the immunity protein resulted in complete protection (*12, 19, 20, 44*). Immunity proteins are located intracellularly, with a very small proportion (~1%) associated with the cell membrane (*20, 45*). CD studies of EntA-im and LeuA-im showed that these proteins are α-helical in water and exposure to membrane mimicking environments did not increase the helicity, implying that the type IIa immunity proteins do not interact strongly with membranes (*12*). Recently, Nes and co-workers used immunoprecipitation experiments to demonstrate that the immunity protein for lactococcin A (not a type IIa immunity protein) forms complexes with the IIC and IID components of the man-PTS complex only in the presence of externally applied lactococcin A. In a similar manner, they explored the interaction of enterocin P and sakacin A with their respective immunity proteins (both group C) and also observed that the flag-tagged immunity proteins formed complexes with the man-PTS system upon exposure to bacteriocin (*24*). This supports the hypothesis that the man-PTS system plays a key role in the mechanism by which immunity proteins protect cells against their bacteriocins (*19, 30*).

Even if immunity is receptor-mediated, it is still unclear whether the immunity protein and bacteriocin interact directly. We have previously used NMR to explore the potential interaction between an immunity protein and its cognate bacteriocin by titrating [$^{15}$N]ImB2 with 1.5 molar equiv of CbnB2. The $^{15}$N HSQC spectrum of ImB2 before and after the addition of CbnB2 showed no changes, thus implying that there was no direct binding between the immunity protein and its bacteriocin (*30*). It has been suggested that a direct interaction may only occur once the bacteriocin is membrane-bound and hence structured (*19*). A recent study by Soliman et al. used molecular dynamics simulations to study the interaction between ImB2 and CbnB2 in a lipid bilayer environment. They reported weak interactions between the immunity protein and bacteriocin (*28*). In this study, we again used NMR to search for an interaction but this time monitored the $^{15}$N HSQC spectrum of the bacteriocin, rather than the immunity protein. Under aqueous conditions, the bacteriocin PisA is unstructured. As expected, the addition of PisI to [$^{15}$N]PisA did not cause significant changes in the $^{15}$N HSQC spectrum, thus indicating that there is no significant interaction. We repeated the experiments under membrane mimicking conditions to see if an interaction could be observed once the bacteriocin had assumed secondary structure. In the presence of TFE, PisA assumed helical structure; however, addition of immunity protein did not result in any further change in the spectrum of PisA. These results suggest that even when the bacteriocin is in the vicinity of the membrane and has assumed secondary structure, there is no significant interaction with the immunity protein that leads to further structuring of the bacteriocin. Thus, the mechanism by which immunity proteins provide protection to producer cells is likely mediated through a putative receptor for the bacteriocin. This receptor appears to be the IIC and/or IID subunits of the mannose phosphotransferase $EII_t^{man}$ system. However, details of the interaction among immunity protein, receptor, and bacteriocin remain elusive.

## CONCLUSIONS

The type IIa immunity proteins are divided into three groups (A, B, and C) based on sequence homology. To date, three type IIa immunity protein structures have been reported: two from group A (EntA-im and PedB) (*31, 32*) and one from group C (ImB2) (*30*). PisI represents the remaining group of these proteins and completes the structural investigation into the type IIa immunity proteins. It is now clear that the four-helix bundle is a conserved structural motif among these immunity proteins. The greatest difference between the group B immunity proteins and the other subgroups is the length of the N-terminus. For the group B immunity proteins, this region may be involved in recognition. Studies involving the activity of either mutant or hybrid proteins, based on the group B proteins, will help elucidate the role of the N-terminus. The details of how immunity proteins protect producer cells remains unclear. Previous studies have shown that the specificity and activity of immunity proteins rely on the C-terminal half of the protein, and it has also been shown that immunity proteins interact with the cytoplasmic portions of the IIC and/or IID components of the $EII_t^{man}$ system. It seems unlikely that there is a direct interaction between immunity protein and bacteriocin in the absence of the receptor protein. Isolation of the IIC and IID components of the $EII_t^{man}$ system and investigations into the interactions of this receptor with bacteriocins and immunity proteins will help reveal the mechanisms of target specificity and immunity.

## ACKNOWLEDGMENT

We are grateful to Dr. Pascal Mercier and Olivier Julien for assistance with CYANA and helpful discussions. We thank Mark Miskolzie (NMR Spectroscopy Laboratory, University of Alberta) for assistance in obtaining the $^{15}$N HSQC spectra of [$^{15}$N]PisA. We also thank Wayne Moffat (Analytical and Instrumentation Laboratory, University of Alberta) for running the CD experiments and Dr. Karen Kawulka for initial work in developing the growth conditions of the MalE−PisI fusion protein.

## SUPPORTING INFORMATION AVAILABLE

Details describing bacterial strains and plasmids (Table SI), primers (Table SII), the expression of [$^{15}$N]PisI and [$^{15}$N]PisA in M9 minimal medium, purification of PisI by

cation-exchange chromatography, purification of PisI by RP-HPLC, and purification of PisI by RP-HPLC and CD spectroscopy, analysis of CD data (Figure S1 and Table SIII), and details of NMR experiments and structural calculations. This material is available free of charge via the Internet at http://pubs.acs.org.

## REFERENCES


1. Cotter, P. D., Hill, C., and Ross, R. P. (2005) Bacteriocins: Developing innate immunity for food. *Nat. Rev. Microbiol. 3*, 777–788.
2. Nes, I. F., Yoon, S. S., and Diep, W. B. (2007) Ribosomally synthesiszed antimicrobial peptides (Bacteriocins) in lactic acid bacteria: A review. *Food Sci. Biotechnol. 16*, 675–690.
3. van Belkum, M. J., and Stiles, M. E. (2000) Nonlantibiotic antibacterial peptides from lactic acid bacteria. *Nat. Prod. Rep. 17*, 323–335.
4. Drider, D., Fimland, G., Héchard, Y., McMullen, L. M., and Prévost, H. (2006) The continuing story of class IIa bacteriocins. *Microbiol. Mol. Biol. Rev. 70*, 564–582.
5. Hastings, J. W., Sailer, M., Johnson, K., Roy, K. L., Vederas, J. C., and Stiles, M. E. (1991) Characterization of leucocin A UAL187 and cloning of the bacteriocin gene from *Leuconostoc gelidum*. *J. Bacteriol. 173*, 7491–7500.
6. Drider, D., Fimland, G., Hechard, Y., McMullen, L. M., and Prevost, H. (2006) The continuing story of class IIa bacteriocins. *Microbiol. Mol. Biol. Rev. 70*, 564–582.
7. Eijsink, V. G. H., Axelsson, L., Diep, D. B., Håvarstein, L. S., Holo, H., and Nes, I. F. (2002) Production of class II bacteriocins by lactic acid bacteria: An example of biological warfare and communication. *Antonie van Leeuwenhoek 81*, 639–654.
8. Gallagher, N. L. F., Sailer, M., Niemczura, W. P., Nakashima, T. T., Stiles, M. E., and Vederas, J. C. (1997) Three-dimensional structure of leucocin A in trifluoroethanol and dodecylphophocholine micelles: Spatial location of residues critical for biological activity in type IIa bacteriocins from lactic acid bacteria. *Biochemistry 36*, 15062–15072.
9. Haugen, H. S., Fimland, G., Nissen-Meyer, J., and Kristiansen, P. E. (2005) Three-dimensional structure in lipid micelles of the pediocin-like antimicrobial peptide curvacin A. *Biochemistry 44*, 16149–16157.
10. Uteng, M., Hauge, H. H., Markwick, P. R. L., Fimland, G., Mantzilas, D., Nissen-Meyer, J., and Muhle-Goll, C. (2003) Three-dimensional structure in lipid micelles of the pediocin-like antimicrobial peptide sakacin P and a sakacin P variant that is structurally stabilized by an inserted C-terminal disulfide bridges. *Biochemistry 42*, 11417–11426.
11. Wang, Y. J., Henz, M. E., Gallagher, N. L. F., Chai, S. Y., Gibbs, A. C., Yan, L. Z., Stiles, M. E., Wishart, D. S., and Vederas, J. C. (1999) Solution structure of carnobacteriocin B2 and implications for structure-activity relationships among type IIa bacteriocins from lactic acid bacteria. *Biochemistry 38*, 15438–15447.
12. Johnsen, L., Fimland, G., Mantzilas, D., and Nissen-Meyer, J. (2004) Structure-function analysis of immunity proteins of pediocin-like bacteriocins: C-terminal parts of immunity proteins are involved in specific recognition of cognate bacteriocins. *Appl. Environ. Microbiol. 70*, 2647–2652.
13. Kaur, K., Andrew, L. C., Wishart, D. S., and Vederas, J. C. (2004) Dynamic relationships among type IIa bacteriocins: Temperature effects on antimicrobial activity and on structure of the C-terminal amphipathic α helix as a receptor-binding region. *Biochemistry 43*, 9009–9020.
14. Fimland, G., Blingsmo, O. R., Sletten, K., Jung, G., Nes, I. F., and NissenMeyer, J. (1996) New biologically active hybrid bacteriocins constructed by combining regions from various pediocin-like bacteriocins: The C-terminal region is important for determining specificity. *Appl. Environ. Microbiol. 62*, 3313–3318.
15. Fimland, G., Eijsink, V. G. H., and Nissen-Meyer, J. (2002) Mutational analysis of the role of tryptophan residues in an antimicrobial peptide. *Biochemistry 41*, 9508–9515.
16. Fimland, G., Jack, R., Jung, G., Nes, I. F., and Nissen-Meyer, J. (1998) The bactericidal activity of pediocin PA-1 is specifically inhibited by a 15-mer fragment that spans the bacteriocin from the center toward the C terminus. *Appl. Environ. Microbiol. 64*, 5057–5060.
17. Fimland, G., Johnsen, L., Axelsson, L., Brurberg, M. B., Nes, I. F., Eijsink, V. G. H., and Nissen-Meyer, J. (2000) A C-terminal disulfide bridge in pediocin-like bacteriocins renders bacteriocin activity less temperature dependent and is a major determinant of the antimicrobial spectrum. *J. Bacteriol. 182*, 2643–2648.
18. Johnsen, L., Fimland, G., and Meyer, J. N. (2005) The C-terminal domain of pediocin-like antimicrobial peptides (class IIa bacteriocins) is involved in specific recognition of the C-terminal part of cognate immunity proteins and in determining the antimicrobial spectrum. *J. Biol. Chem. 280*, 9243–9250.
19. Fimland, G., Eijsink, V. G. H., and Nissen-Meyer, J. (2002) Comparative studies of immunity proteins of pediocin-like bacteriocins. *Microbiology 148*, 3661–3670.
20. Quadri, L. E. N., Kleerebezem, M., Kuipers, O. P., DeVos, W. M., Roy, K. L., Vederas, J. C., and Stiles, M. E. (1997) Characterization of a locus from *Carnobacterium piscicola* LV17B involved in bacteriocin production and immunity: Evidence for global inducer-mediated transcriptional regulation. *J. Bacteriol. 179*, 6163–6171.
21. Franz, C., van Belkum, M. J., Worobo, R. W., Vederas, J. C., and Stiles, M. E. (2000) Characterization of the genetic locus responsible for production and immunity of carnobacteriocin A: The immunity gene confers cross-protection to enterocin B. *Microbiology 146*, 621–631.
22. Yan, L. Z., Gibbs, A. C., Stiles, M. E., Wishart, D. S., and Vederas, J. C. (2000) Analogues of bacteriocins: Antimicrobial specificity and interactions of leucocin A with its enantiomer, carnobacteriocin B2, and truncated derivatives. *J. Med. Chem. 43*, 4579–4581.
23. Dalet, K., Cenatiempo, Y., Cossart, P., Consortium, E. L. G., and Héchard, Y. (2001) A $\sigma^{54}$-dependent PTS permease of the mannose family is responsible for sensitivity of *Listeria monocytogenes* to mesentericin Y105. *Microbiology 147*, 3263–3269.
24. Diep, D. B., Skaugen, M., Salehian, Z., Holo, H., and Nes, I. F. (2007) Common mechanisms of target cell recognition and immunity for class II bacteriocins. *Proc. Natl. Acad. Sci. U.S.A. 104*, 2384–2389.
25. Gravesen, A., Ramnath, M., Rechinger, K. B., Andersen, N., Jänsch, L., Héchard, Y., Hastings, J. W., and Knøchel, S. (2002) High-level resistance to class IIa bacteriocins is associated with one general mechanism in *Listeria monocytogenes*. *Microbiology 148*, 2361–2369.
26. Héchard, Y., Pelletier, C., Cenatiempo, Y., and Frère, J. (2001) Analysis of σ54-dependent genes in *Enterococcus faecalis*: A mannose PTS permease ($EII^{Man}$) is involved in sensitivity to a bacteriocin, mesentericin Y105. *Microbiology 147*, 1575–1580.
27. Ramnath, M., Beukes, M., Tamura, K., and Hastings, J. W. (2000) Absence of a putative mannose-specific phosphotransferase system enzyme IIAB component in a leucocin A resistant strain of *Listeria monocytogenes*, as shown by two-dimensional sodium dodecyl sulfate-polyacrylamide gel electrophoresis. *Appl. Environ. Microbiol. 66*, 3098–3101.
28. Soliman, W., Bhattacharjee, S., and Kaur, K. (2007) Molecular dynamics simulation study of interaction between a class IIa bacteriocin and its immunity protein. *Biochim. Biophys. Acta 1774*, 1002–1013.
29. Sprules, T., Kawulka, K. E., Gibbs, A. C., Wishart, D. S., and Vederas, J. C. (2004) NMR solution structure of the precursor for carnobacteriocin B2, an antimicrobial peptide from *Carnobacterium piscicola*: Implications of the α-helical leader section for export and inhibition of type IIa bacteriocin activity. *Eur. J. Biochem. 271*, 1748–1756.
30. Sprules, T., Kawulka, K. E., and Vederas, J. C. (2004) NMR solution structure of ImB2, a protein conferring immunity to antimicrobial activity of the type IIa bacteriocin, carnobacteriocin B2. *Biochemistry 43*, 11740–11749.
31. Johnsen, L., Dalhus, B., Leiros, I., and Nissen-Meyer, J. (2005) 1.6 Å crystal structure of EntA-im: A bacterial immunity protein conferring immunity to the antimicrobial activity of the pediocin-like bacteriocin enterocin A. *J. Biol. Chem. 280*, 19045–19050.
32. Kim, I. K., Kim, M. K., Kim, J. H., Yim, H. S., Cha, S. S., and Kang, S. O. (2007) High resolution crystal structure of PedB: A structural basis for the classification of pediocin-like immunity proteins. *BMC Struct. Biol. 7*, 35–43.
33. Gursky, L. J., Martin, N. I., Derksen, D. J., van Belkum, M. J., Kaur, K., Vederas, J. C., Stiles, M. E., and McMullen, L. M. (2006) Production of piscicolin 126 by *Carnobacterium maltaromaticum* UAL26 is controlled by temperature and induction peptide concentration. *Arch. Microbiol. 186*, 317–325.
34. Jack, R. W., Wan, J., Gordon, J., Harmark, K., Davidson, B. E., Hillier, A. J., Wettenhall, R. E. H., Hickey, M. W., and Coventry,

M. J. (1996) Characterization of the chemical and antimicrobial properties of piscicolin 126, a bacteriocin produced by *Carnobacterium piscicola* JG126. *Appl. Environ. Microbiol. 62*, 2897–2903.
35. Delaglio, F., Grzesiek, S., Vuister, G. W., Zhu, G., Pfeifer, J., and Bax, A. (1995) NMRPipe: A multidimensional spectral processing system based on Unix pipes. *J. Biomol. NMR 6*, 277–293.
36. Johnson, B. A., and Blevins, R. A. (1994) NMR View: A computer program for the visualization and analysis of NMR data. *J. Biomol. NMR 4*, 603–614.
37. Güntert, P., Mumenthaler, C., and Wüthrich, K. (1997) Torsion angle dynamics for NMR structure calculation with the new program DYANA. *J. Mol. Biol. 273*, 283–298.
38. Koradi, R., Billeter, M., and Wüthrich, K. (1996) MOLMOL: A program for display and analysis of macromolecular structures. *J. Mol. Graphics 14*, 51–55.
39. Dolinsky, T. J., Nielsen, J. E., McCammon, J. A., and Baker, N. A. (2004) PDB2PQR: An automated pipeline for the setup of Poisson-Boltzmann electrostatics calculations. *Nucleic Acids Res. 32*, 665–667.
40. Baker, N. A., Sept, D., Joseph, S., Holst, M. J., and McCammon, J. A. (2001) Electrostatics of nanosystems: Application to microtubules and the ribosome. *Proc. Natl. Acad. Sci. U.S.A. 98*, 10037–10041.
41. Gasteiger, E., Hoogland, C., Gattiker, A., Duvaud, S., Wilkins, M. R., Appel, R. D., and Bairoch, A. (2005) Protein identification and analysis tools on the ExPASy server, in *The Proteomics Protocols Handbook* (Walker, J. M., Ed.) pp 571−607, Humana Press, Totowa, NJ.
42. Wishart, D. S., and Sykes, B. D. (1994) The $^{13}C$ Chemical-Shift Index: A simple method for the identification of protein secondary structure using $^{13}C$ chemical-shift data. *J. Biomol. NMR 4*, 171–180.
43. Quadri, L. E. N., Sailer, M., Terebiznik, M. R., Roy, K. L., Vederas, J. C., and Stiles, M. E. (1995) Characterization of the protein conferring immunity to the antimicrobial peptide carnobacteriocin B2 and expression of carnobacteriocins B2 and BM1. *J. Bacteriol. 177*, 1144–1151.
44. Eijsink, V. G. H., Skeie, M., Middelhoven, P. H., Brurberg, M. B., and Nes, I. F. (1998) Comparative studies of class IIa bacteriocins of lactic acid bacteria. *Appl. Environ. Microbiol. 64*, 3275–3281.
45. Dayem, M. A., Fleury, Y., Devilliers, G., Chaboisseau, E., Girard, R., Nicolas, P., and Delfour, A. (1996) The putative immunity protein of the Gram-positive bacteria *Leuconostoc mesenteroides* is preferentially located in the cytoplasm compartment. *FEMS Microbiol. Lett. 138*, 251–259.
46. Thompson, J. D., Higgins, D. G., and Gibson, T. J. (1994) CLUSTAL W: Improving the sensitivity of progressive multiple sequence alignment through sequence weighting, position-specific gap penalties and weight matrix choice. *Nucleic Acids Res. 22*, 4673–4680.
47. Fremaux, C., Héchard, Y., and Cenatiempo, Y. (1995) Mesentericin Y105 gene clusters in *Leuconostoc mesenteroides* Y105. *Microbiology 141*, 1637–1645.
48. O'Keeffe, T., Hill, C., and Ross, R. P. (1999) Characterization and heterologous expression of the genes encoding enterocin A production, immunity, and regulation in *Enterococcus faecium* DPC1146. *Appl. Environ. Microbiol. 65*, 1506–1515.
49. Métivier, A., Pilet, M. F., Dousset, X., Sorokine, O., Anglade, P., Zagorec, M., Piard, J. C., Marion, D., Cenatiempo, Y., and Fremaux, C. (1998) Divercin V41, a new bacteriocin with two disulphide bonds produced by *Carnobacterium divergens* V41: Primary structure and genomic organization. *Microbiology 144*, 2837–2844.
50. Brurberg, M. B., Nes, I. F., and Eijsink, V. G. H. (1997) Pheromone-induced production of antimicrobial peptides in *Lactobacillus*. *Mol. Microbiol. 26*, 347–360.
51. Kawamoto, S., Shima, J., Sato, R., Eguchi, T., Ohmomo, S., Shibato, J., Horikoshi, N., Takeshita, K., and Sameshima, T. (2002) Biochemical and genetic characterization of mundticin KS, an antilisterial peptide produced by *Enterococcus mundtii* NFRI 7393. *Appl. Environ. Microbiol. 68*, 3830–3840.
52. Saavedra, L., de Ruiz Holgado, A., and Sesma, F. (2003) GenBank entry AY398693.
53. Kalmokoff, M. L., Banerjee, S. K., Cyr, T., Hefford, M. A., and Gleeson, T. (2001) Identification of a new plasmid-encoded *sec*-dependent bacteriocin produced by *Listeria innocua* 743. *Appl. Environ. Microbiol. 67*, 4041–4047.
54. Vaughan, A., Eijsink, V. G. H., and van Sinderen, D. (2003) Functional characterization of a composite bacteriocin locus from malt isolate *Lactobacillus sakei* 5. *Appl. Environ. Microbiol. 69*, 7194–7203.
55. Tichaczek, P. S., Vogel, R. F., and Hammes, W. P. (1994) Cloning and sequencing of *sakP* encoding sakacin P, the bacteriocin produced by *Lactobacillus sake* ITH 673. *Microbiology 140*, 361–367.
56. Quadri, L. E. N., Sailer, M., Roy, K. L., Vederas, J. C., and Stiles, M. E. (1994) Chemical and genetic characterization of bacteriocins produced by *Carnobacterium piscicola* LV17B. *J. Biol. Chem. 269*, 12204–12211.
57. Axelsson, L. (2004) GenBank entry AJ626711.
58. Cintas, L. M., Casaus, P., Håvarstein, L. S., Hernández, P. E., and Nes, I. F. (1997) Biochemical and genetic characterization of enterocin P, a novel *sec*-dependent bacteriocin from *Enterococcus faecium* P13 with a broad antimicrobial spectrum. *Appl. Environ. Microbiol. 63*, 4321–4330.
59. Axelsson, L., and Holck, A. (1995) The genes involved in production of and immunity to sakacin A, a bacteriocin from *Lactobacillus sake* Lb706. *J. Bacteriol. 177*, 2125–2137.
60. Tomita, H., Fujimoto, S., Tanimoto, K., and Ike, Y. (1996) Cloning and genetic organization of the bacteriocin 31 determinant encoded on the *Enterococcus faecalis* pheromone responsive conjugative plasmid pYI17. *J. Bacteriol. 178*, 3585–3593.

BI8004076